

A GIS-based comparative study of frequency ratio, statistical index and weights-of-evidence models in landslide susceptibility mapping

Wei Chen¹ · Huichan Chai² · Xueyang Sun¹ · Qiqing Wang² · Xiao Ding³ · Haoyuan Hong⁴

Received: 14 January 2015 / Accepted: 18 September 2015 / Published online: 10 March 2016
© Saudi Society for Geosciences 2016

Abstract The aim of this study is to generate reliable susceptibility maps using frequency ratio (FR), statistical index (SI), and weights-of-evidence (WoE) models based on geographic information system (GIS) for the Qianyang County of Baoji City, China. At first, landslide locations were identified by earlier reports, aerial photographs, and field surveys, and a total of 81 landslides were mapped from various sources. Then, the landslide inventory was randomly split into a training dataset 70 % (56 landslides) for training the models, and the remaining 30 % (25 landslides) was used for validation purpose. In this case study, 13 landslide-conditioning factors were exploited to detect the most susceptible areas. These factors are slope angle, slope aspect, curvature, plan curvature, profile curvature, altitude, distance to faults, distance to rivers, distance to roads, Sediment Transport Index (STI), Stream Power Index (SPI), Topographic Wetness Index (TWI), and lithology. Subsequently, landslide-susceptible areas were mapped using the FR, SI, and WoE models based on landslide-conditioning factors. Finally, the accuracy of the landslide susceptibility maps produced from the three models was verified by using areas under the curve (AUC). The AUC plot estimation results showed that the susceptibility map

using FR model has the highest training accuracy of 83.62 %, followed by the SI model (83.45 %), and the WoE model (82.51 %). Similarly, the AUC plot showed that the prediction accuracy of the three models was 79.40 % for FR model, 79.35 % for SI model, and 78.53 % for WoE model, respectively. According to the validation results of the AUC evaluation, the map produced by FR model exhibits the most satisfactory properties.

Keywords Landslide · Statistical model · Areas under the curve (AUC) · Qianyang county · China

Introduction

Landslides, resulting in significant damage to people and property, are one of the most costly and damaging geological hazards in many areas of the world. The frequency of landslide occurrences increases with growing human population. Globally, landslides cause hundreds of billions of dollars in damage, thousands of casualties and fatalities, and environmental losses each year (Aleotti and Chowdhury 1999). In China, more than 10,000 hazards associated with landslides occurred in 2014, which caused a total of 400 people dead or missing, 218 people injured, and a direct economic loss of 5.41 billion CNY (C.H. of China geological environment information sit (CIGEM) 2014). Currently, tens of millions of people still live under the high-risk threat of landslides (Liu et al. 2013).

In general, landslide susceptibility mapping, defined as qualitative methods which are direct hazard mapping techniques or quantitative methods which are indirect mapping techniques (Fell et al. 2008; Grozavu et al. 2013; Kayastha et al. 2013; Youssef et al. 2014a, b; Jaupaj et al. 2014), relies on a rather complex knowledge of slope movements and their controlling factors. The reliability of landslide susceptibility

✉ Wei Chen
chenwei.0930@163.com

¹ School of Geology and Environment, Xi'an University of Science and Technology, Xi'an 710054, China

² School of Resources and Earth Science, China University of Mining and Technology, Xuzhou 221116, China

³ College of Architecture and Civil Engineering, Xi'an University of Science and Technology, Xi'an 710054, China

⁴ Jiangxi Provincial Meteorological Observatory, Jiangxi Meteorological Bureau, Nanchang 330046, China

maps mainly depends on the amount and quality of available data, the working scale, and the selection of the appropriate methodology of analysis and modeling (Baeza and Corominas. 2001). Over the last decades, there have been studies on landslide susceptibility evaluation using GIS, and many of these studies have applied probabilistic models (Lee and Min 2001; Baeza and Corominas 2001; Dahal et al. 2008; Pradhan et al. 2006, 2011; Youssef et al. 2009, 2012; Cevik and Topal 2003; Pradhan and Youssef 2010; Vijith and Madhu 2008; Clerici et al. 2002, 2006; Donati and Turrini 2002; Luzi et al. 2000; Jibson et al. 2000; Zhou et al. 2002; Parise and Jibson 2000; Lee and Choi 2003; Lee et al. 2004a, b; Akgun et al. 2012a; Pareek et al. 2013; Kayastha 2015; Youssef et al. 2015a, b). The statistical models available, such as the logistic regression models (Bathrellos et al. 2009; Akgun 2012; Tunusluoglu et al. 2007; Xu et al. 2012b; Devkota et al. 2013; Ozdemir and Altural 2013; Kundu et al. 2013; Park et al. 2013; Grozavu et al. 2013) and bivariate models (Pradhan and Youssef 2010; Pareek et al. 2010; Pradhan and Lee 2010; Pourghasemi et al. 2013a), has also been applied to landslide susceptibility mapping. As other different methods such as certainty factor (CF) (Devkota et al. 2013; Pourghasemi et al. 2013b), analytical hierarchy process (AHP) (Rozos et al. 2011; Bathrellos et al. 2012, 2013; Pourghasemi et al. 2012, 2013a; Park et al. 2013; Youssef et al. 2014a, b), spatial multicriteria decision analysis (MCDA) (Akgun and Turk 2010; Akgun 2012), weights of evidence (WoE) (Ozdemir and Altural 2013; Pourghasemi et al. 2013b, c; Regmi et al. 2014), statistical index (SI) (Bui et al. 2011; Regmi et al. 2014), index of entropy (IoE) model (Mihaela et al. 2011; Devkota et al. 2013), artificial neural network (ANN) (Nefeslioglu et al. 2008; Poudyal et al. 2010; Yilmaz 2009a, b, 2010a, b), fuzzy logic (Akgun et al. 2012b; Pourghasemi et al. 2012; Sharma et al. 2013; Guettouche 2013), support vector machine (SVM) (Yilmaz 2010b; Marjanović et al. 2011; Xu et al. 2012a; Pradhan 2013), and decision tree (Pradhan 2013) have also been applied for landslide susceptibility evaluation. All these models provide solutions for integrating information levels and mapping the outputs.

The aim of the present study was to produce landslide susceptibility maps of Qianyang County in Baoji, China (Fig. 1). For this purpose, landslide-related data have been collected and constructed to spatial database; landslide-related factors have been extracted and overlaid using three statistical models: frequency ratio (FR), statistical index (SI), and weights-of-evidence (WoE) models in order to find the best model that is more accurate in landslide susceptibility mapping in the study area. These models exploit information obtained from an inventory map to offer a guide of landslide inventory or of landslide-prone area, in order to efficiently mitigate the hazard and even avoid the hazard in future. To evaluate the accuracy of three models, the landslide susceptibility analysis results were validated by comparing with the

existing landslide locations according to the area under the curve (AUC). The models' prediction capabilities were tested.

The main difference between the present study and the approaches described in the aforementioned publications is that the frequency ratio (FR), statistical index (SI), and weights-of-evidence (WoE) models were applied, and their results were compared for landslide susceptibility at the study area for the first time.

Study area

The study area is located in Qianyang County of Baoji City, China, between latitudes 34°34'34" to 34°56'56"N and longitudes 106°56'15" to 107°22'31"E (Fig. 1). It covers roughly a surface area of 996.46 km². The altitude of the area ranges from 752 to 1560 m a.s.l and decreases from the north to the south. The landform can be classified into mountain, hill, and plain. The slope angles of the area range from 0° to as much as 38°. The rivers of the study area are belonging to Wei and Jing river basins. The mean annual rainfall according to local station in a period of 40 years is around 627.4 mm. Also, based on the records from China's meteorological department (C.H. of China Meteorological Administration (CMA) 2014), the minimum and maximum rainfall occurs in January and September, respectively. The average mean annual temperature is 11.8 °C. The stratigraphic column of the study area is shown in Fig. 2. The study area is mainly distributed by loess and 81 landslides distributed in the study area. Figure 3 shows significant photographs of landslides occurred in the study area.

Methodology

Frequency ratio model

The frequency ratio (FR) approach, a variant of the probabilistic method, is based on the observed relationships between the distribution of landslides and each landslide conditioning factor (Tay et al. 2014). The frequency ratios for the class or type of each conditioning factor were calculated by dividing the landslide occurrence ratio by the area ratio. The landslide susceptibility index (LSI) was calculated by summation of each factor's ratio value using Eq. (1) (Lee and Talib 2005):

$$LSI = \sum FR \quad (1)$$

where, LSI is the landslide susceptibility index. FR is the frequency ratio of each factor type or class.

Statistical index model

The statistical index approach, a bivariate statistical analysis, is considered as the simplest and quantitatively suitable method in landslide susceptibility mapping. In this method, the weighting value for each categorical unit is defined as the natural logarithm of the landslide density in a class divided by the landslide density in the whole studied area (Bourenane et al. 2015; Pourghasemi et al. 2013a). This method is based on the following equation:

$$W_{ij} = \ln\left(\frac{D_{ij}}{D}\right) = \ln\left[\left(\frac{N_{ij}/N}{S_{ij}/S}\right)\right] \tag{2}$$

where W_{ij} is the weight given to a certain class i of parameter j , D_{ij} is the landslide density within class i of parameter j , D is the total landslide density within the entire map, N_{ij} is the number of landslides in a certain class i of parameter j , S_{ij} is the number of pixels in a certain class i of parameter j , N is the total number of landslides in the entire map, and S is the total pixels of the entire map.

Weights-of-evidence model

Weights-of-evidence (WoE), based on Bayesian Bayes' theorem and assessing the relation between the spatial distribution of the areas affected by landslides and the spatial distribution of the conditioning factors causing landslides, is one of the bivariate models (Sujatha et al. 2014; Dahal et al. 2008). The WoE model is fundamentally based on the calculation of positive and negative weights W^+ and W^- . The positive and negative weights (W_i^+ and W_i^-) are assigned to each of the different classes of causative factor (Van Westen et al. 2003), and positive and negative weights are defined as:

$$W_i^+ = \ln \frac{P\{B|D\}}{P\{B|\bar{D}\}} \tag{3}$$

$$W_i^- = \ln \frac{P\{\bar{B}|D\}}{P\{\bar{B}|\bar{D}\}} \tag{4}$$

where P is the probability and \ln is the natural log, B is the presence of potential landslide causative factor, \bar{B} is the absence of a potential landslide causative factor, D is the presence of landslide, and \bar{D} is the absence of a landslide. W_i^+ and W_i^- are the weights-of-evidence when the causative variable is present and absent at the landslide locations,

respectively (Dahal et al. 2008; Oh and Lee 2011). The standard deviation of W is calculated as:

$$S(C) = \sqrt{S^2 W^+ + S^2 W^-} \tag{5}$$

where $S^2(W^+)$ and $S^2(W^-)$ are variances of W^+ and W^- , respectively. The difference between the two weights is known as the weight contrast, $C(C = W_i^+ - W_i^-)$. $C/S(C)$ provides a measure of the strength of the correlation between the analyzed variable and landslides (Dahal et al. 2008; Kouli et al. 2014).

Conditioning factors database

Landslide inventory

Historic information on landslide occurrences, giving shrewdness into the frequency, volumes, damages, and types of the landslide phenomena, is the backbone of landslide susceptibility studies (Youssef et al. 2015a, b; van Westen et al. 2006). Landslide inventories are the ones that collect the data including information related to topics such as the regional landslide locations, types, activities, and physical properties, usually mapped with an associated database (Fell et al. 2008; Demir et al. 2015). A landslide inventory map provides the basic information for evaluating landslide hazards or risks. Accurate collection of the data related to landslides is very important for landslide susceptibility analysis. In order to produce a detailed and reliable landslide inventory map, extensive field surveys and observations were performed in the study area. A total of 81 landslides (71 earth slide and 10 earth fall) were identified and mapped by evaluating aerial photos in 1:50,000 scale with well supported by field surveys and subsequently digitized for further analysis. The DEM of the study was generated from topographic maps in 1:10,000 scale with a contour interval of 10 m. The locations (centroid) of 81 landslides are mapped in Fig. 1. From these landslides, 56 (70 %) randomly selected were taken for making landslide susceptibility models, and 25 (30 %) were used for validating the models. The study area was divided into a grid with 50 × 50-m cell, occupying 984 rows and 1146 columns.

Landslide-conditioning factors

In the study, 13 landslide-conditioning factors (slope angle, slope aspect, curvature, plan curvature, profile curvature, altitude, distance to faults, distance to rivers, distance to roads, STI, SPI, TWI, and lithology) were considered during the landslide susceptibility mapping of the study area. All the data used in the current study were georeferenced to Gauss_Kruger coordinate system, D_Beijing_1954 datum, and zone 18 N.

Fig. 1 Location map of the study area

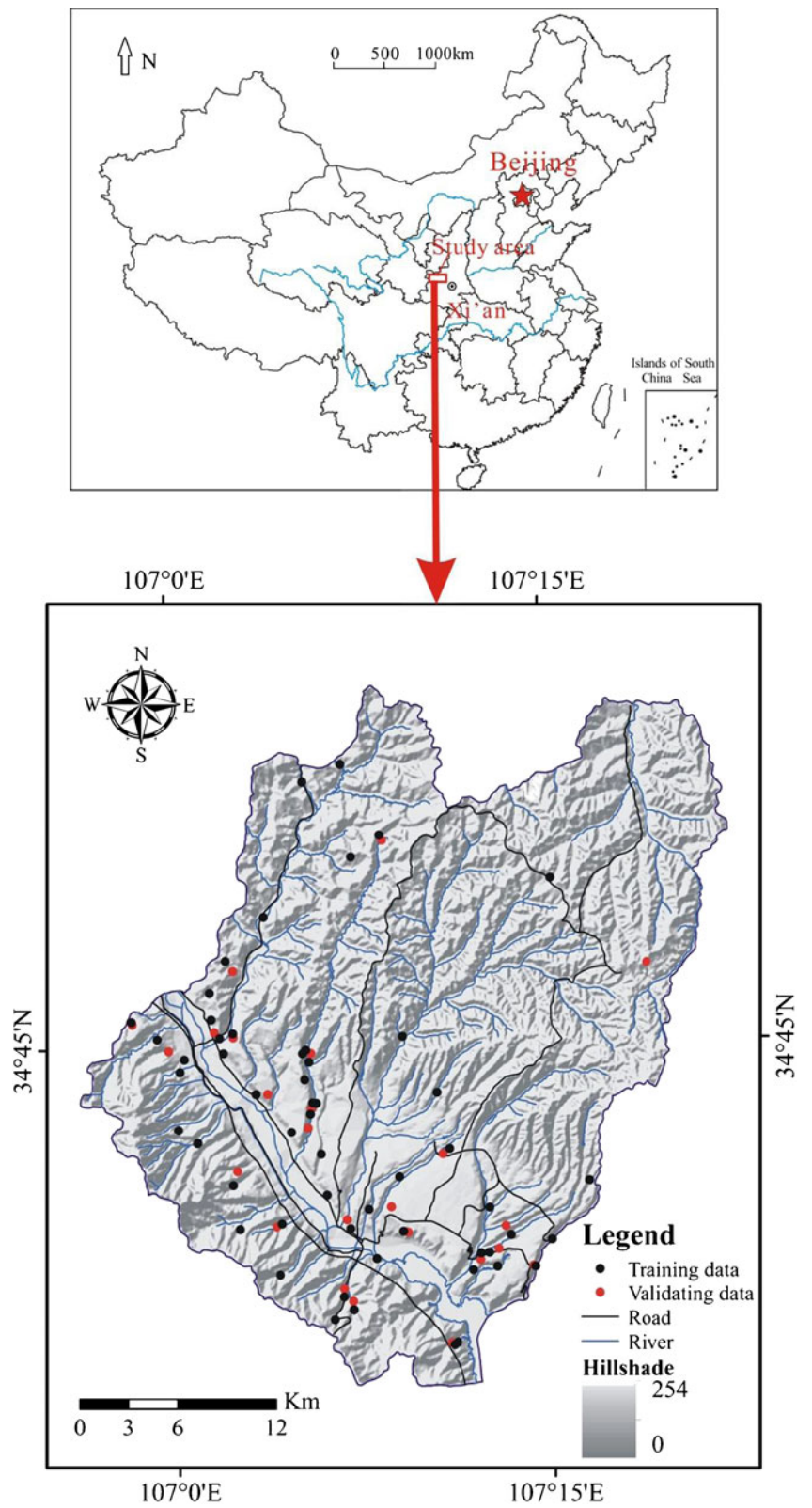


Fig. 2 The stratigraphic column of the study area

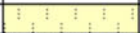
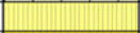


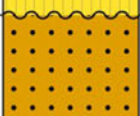





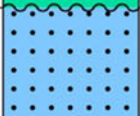


Sys.	Ser.	Fm.	Code	Column	Description
Quaternary	Holocene	—	Q ₄		Sand, gravel, silty clay
	Pleistocene	—	Q ₃		Loess
	Pleistocene	—	Q ₂		Loess
	Pleistocene	—	Q ₁		Loess
Neogene	Pliocene	—	N ₂		Glutenite, sandstone, siltstone
Cretaceous	Lower	Luohandong	K _{1LH}		Sandstone, siltstone, mudstone
		Huanhehuachi	K _h		Sandstone, siltstone, mudstone
		Luohe	K _{1L}		Glutenite, sandstone
		Yijun	K _{1y}		Glutenite
Jurassic	Upper	Fenfanghe	J _{3f}		Glutenite, sandstone, siltstone
	Middle	Zhiluo	J _{2z}		Glutenite, siltstone
Permian	Lower	—	P ₁		Sandstone, shale
Ordovician	Middle Lower	—	O ₁₋₂		Limestone, dolomite

Fig. 3 Field photographs of the study area



These factors fall under the category of preparatory factors, responsible for the occurrence of landslides in the region for which pertinent data can be collected from available resources as well as from the field surveys.

Slope angle

Slope angle is an important factor in the assessment of slope stability, and it is frequently used in preparing landslide susceptibility maps (Lee and Min 2001; Saha et al. 2005). The slope angle map of the study area is prepared from the digital elevation model (DEM) and was reclassified into five equal classes as 0–7, 7–14, 14–21, 21–28, and 28–38° (Fig. 4a).

Slope aspect

Slope aspect, accepted as a landslide-conditioning factor, describes the direction of slope (Ercanoglu et al. 2004; Pourghasemi et al. 2012). The slope aspect of the study area (Fig. 4b) is divided into eight directional classes as flat (–1), north (337.5–360°, 0–22.5°), northeast (22.5–67.5°), east (67.5–112.5°), southeast (112.5–157.5°), south (157.5–202.5°), southwest (202.5–247.5°), west (247.5–292.5°), and northwest (292.5–337.5°).

Curvature

Generally, curvature is defined as the rate of change of slope angle or aspect, and the characterization of slope morphology and flow can be analyzed with the help of the curvature map (Nefeslioglu et al. 2008; Catani et al. 2013). In this study, the curvature which is the combination of plane and profile curvature is taken into consideration (Fig. 4c). The curvature was derived from the DEM in Geographic information system software of ArcGIS 10.0 and divided into three classes: <math><-0.05</math>, $-0.05-0.05$, and >0.05, respectively.

Plan curvature

Plan curvature is the curvature of a contour line formed by intersecting a horizontal plane with the surface. Plan curvature

influences the convergence or divergence of water during downhill flow (Yilmaz et al. 2012). In this study, the plan curvature was derived from the DEM in Geographic information system software of ArcGIS 10.0 and divided into three classes: <math><-0.05</math>, $-0.05-0.05$, and >0.05, respectively (Fig. 4d).

Profile curvature

Profile curvature is the curvature in the vertical plane parallel to the slope direction. It measures the rate of change of slope. Therefore, it influences the flow velocity of water draining the surface and thus erosion and the resulting down slope movement of sediment (Yilmaz and Topal 2012). In this study, the profile curvature was also derived from the DEM in Geographic information system software of ArcGIS 10.0 and divided into three classes: <math><-0.05</math>, $-0.05-0.05$, and >0.05, respectively (Fig. 4e).

Altitude

Altitude or elevation is another frequently used conditioning factor for landslide susceptibility analysis. In the present study, the DEM of the study was generated from topographic maps in 1:10,000 scale with a contour interval of 10 m. The elevation of the study area ranged from 720 to 1560 m. The elevation values were divided into five categories using an interval of 150 m (Fig. 4f).

Distance to faults

Geological faults are responsible for triggering a large number of landslides due to the tectonic breaks that usually decrease the rock strength. In the study area, the faults of the study area were digitized from the geological map with 1:250,000 scale. The distance to faults is calculated at 2000-m intervals using the geological map (Fig. 4g).

Distance to rivers

Runoff plays an important role as a triggering factor for landslides due to rivers are the main mechanisms that contribute to the occurrence of landslides in mountainous regions (Park et al. 2013). For the current study, six different buffer

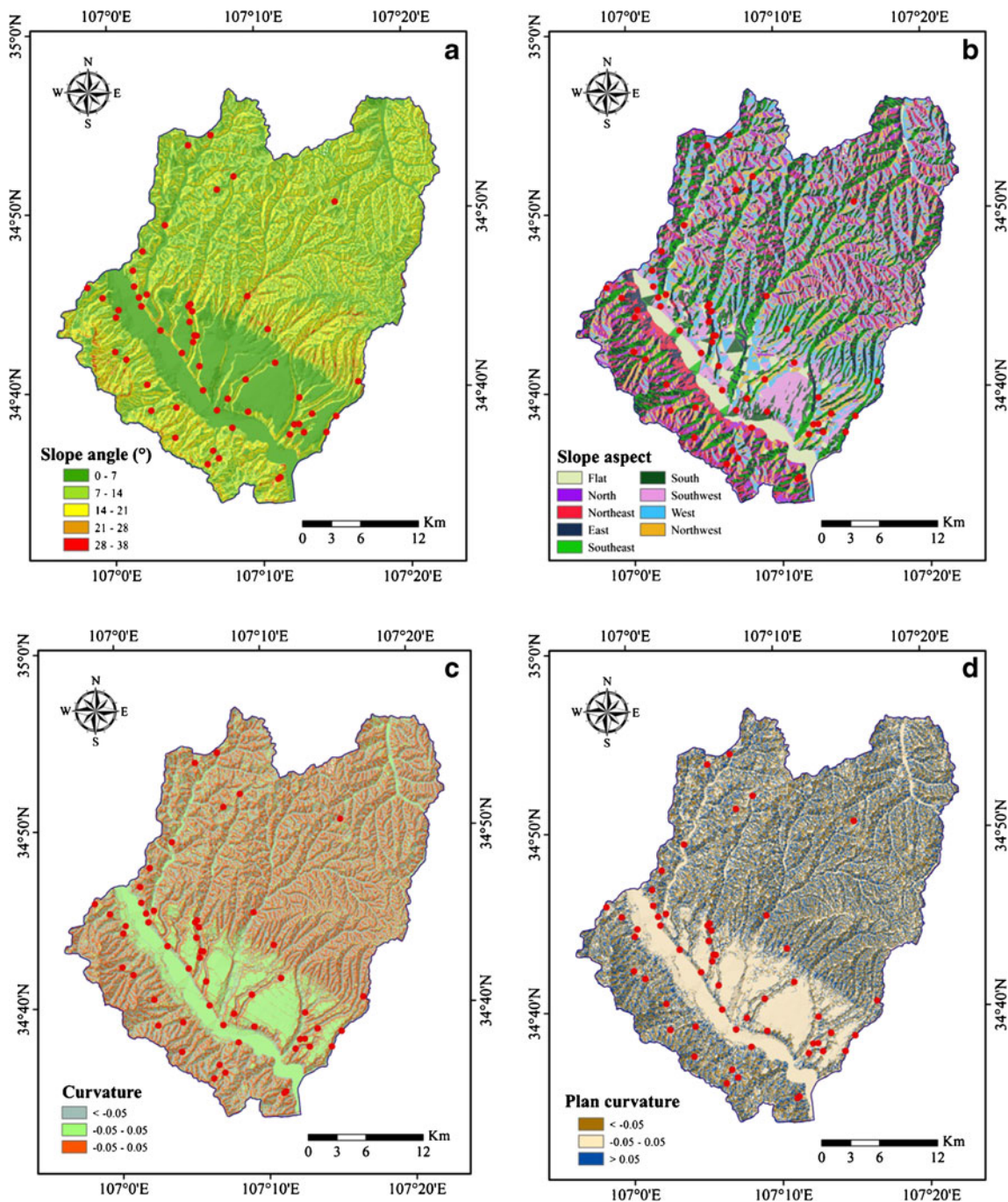


Fig. 4 Landslide-conditioning factors of the study area. **a** slope angle, **b** slope aspect, **c** curvature, **d** plan curvature, **e** profile curvature, **f** altitude, **g** distance to faults, **h** distance to rivers, **i** distance to roads, **j** STI, **k** SPI, **l** TWI, **m** lithology

categories were created within the study area to determine the degree to which the streams affected the slopes (Fig. 4h).

Distance to roads

The distance to roads has been considered as one of the most important anthropogenic factors influencing landslides occurrence that can be the cause of cut slope creations through construction of roads that disturbs the natural topology and

affects the stability of the slope. The study area was divided into five different buffer zones to designate the influence of the road on slope stability (Fig. 4i): 0–1,000 m, 1000–2000, 2000–3000, 3000–4000 and >4000 m.

STI

The sediment transport index (STI) is characterized by the process of erosion and deposition (Devkota et al. 2013). In

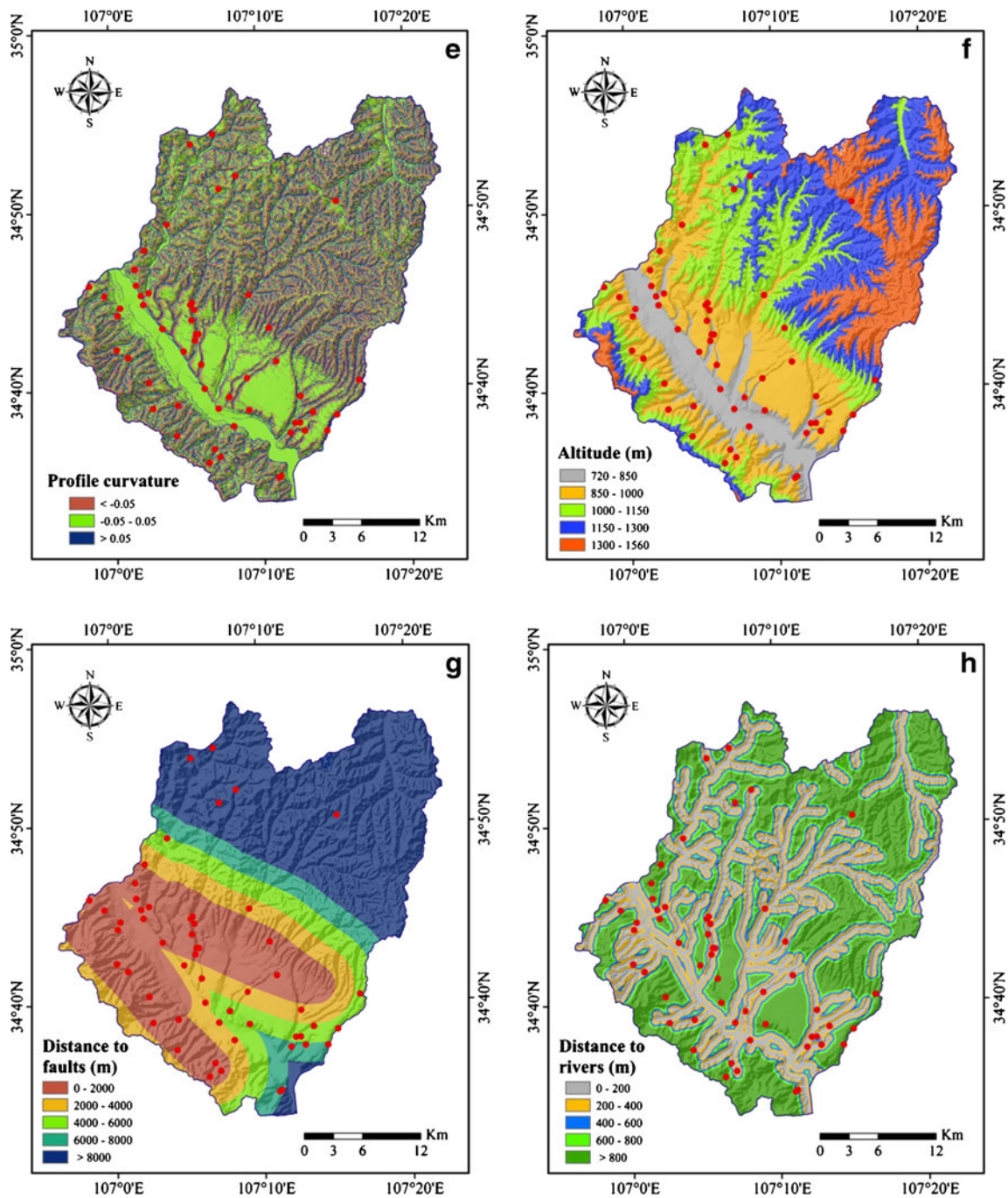


Fig. 4 (continued)

the present study, STI is divided into four classes <3, 3–9, 9–15, >15 (Fig. 4j).

SPI

The stream power index (SPI), a measure of the erosive power of water flow based on the assumption that discharge is proportional to the specific catchment area, is a compound topographic attribute (Conforti et al. 2011). The SPI map of

the study area was classified into four classes: <5, 5–10, 10–40, and >40 (Fig. 4k).

TWI

The topographic wetness index (TWI) is another topographic factor within the runoff model (Pourghasemi et al. 2013d). In the present study, the TWI values, derived from the DEM,

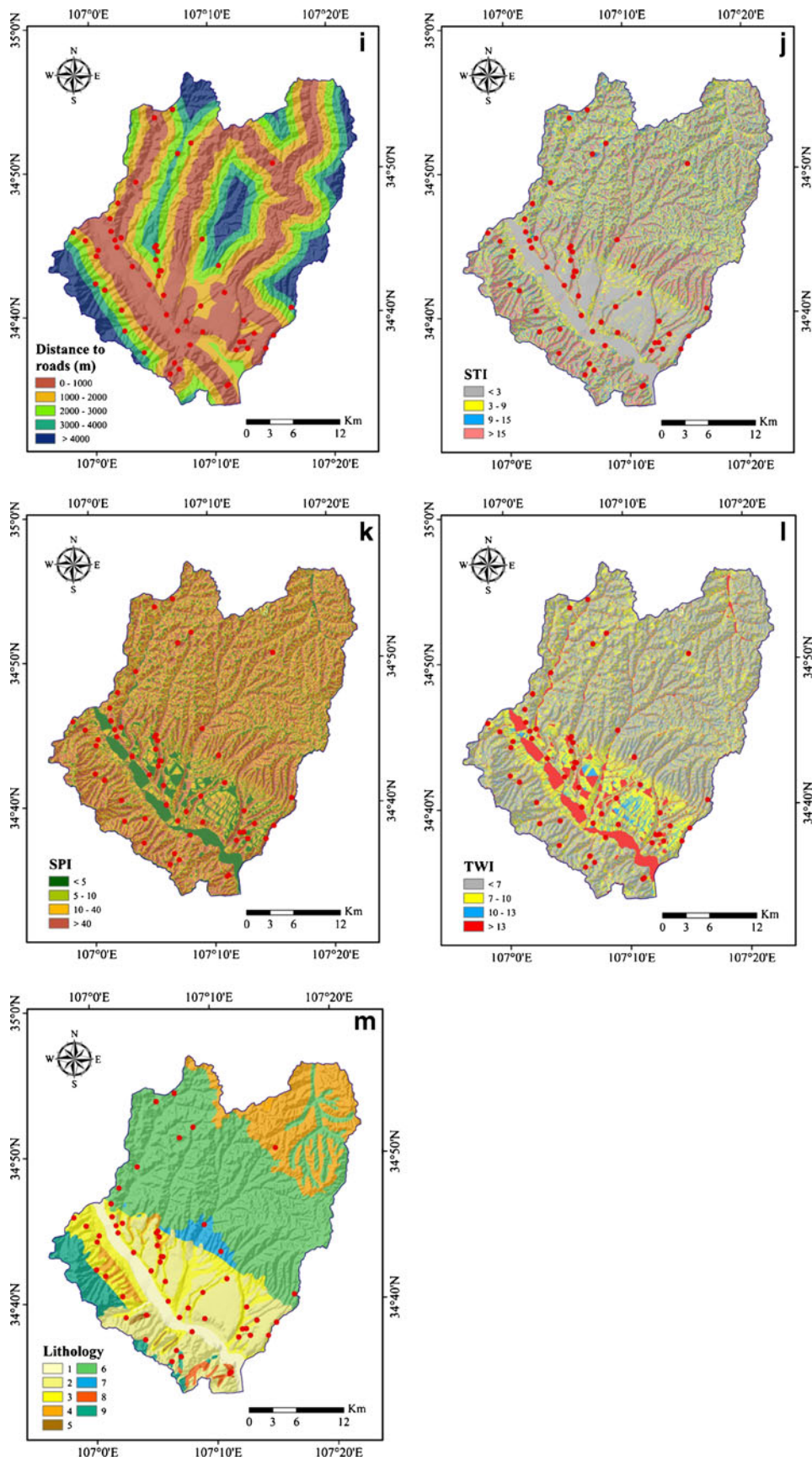


Fig. 4 (continued)

were arranged in four classes: <7, 7–10, 10–13, and >13 (Fig. 4l).

Lithology

Lithology is one of the most common determinant factors in most landslide stability studies. Since different lithological units have different landslide susceptibility values, they are very important in providing data for susceptibility studies. The lithology map of the study area is derived from existing geological maps in 1:250,000 scale. The study area is covered with various types of lithological units. Their names, lithologic characteristics, and ages of the geological units are provided in Table 1. As shown in Fig. 4m.

Results and discussion

Frequency ratio model

Using the frequency ratio model, frequency ratios for the class or type of each factor were calculated by dividing the landslide occurrence ratio by the area ratio. A frequency ratio value of 1 is an average value for the area landslides occurring in the total area. A frequency ratio value less than 1 indicates a lower correlation which indicates a high probability of landslide occurrence, and a weight value greater than 1 indicates a higher probability of landslide occurrence. The FR of all the thematic layers used in the present study was calculated in ArcGIS 10.0 and Microsoft Excel, and the result is given in Table 2.

A landslide susceptibility map (Fig. 5) was constructed using the LSI value by the software of ArcGIS 10.0. The calculated LSI values for FR model of the study area range from about 6.59 to 25.32. Obviously, larger LSI values indicate a higher susceptibility for landsliding. The index values were classified into five zones (very low, low, moderate, high,

and very high) using the natural break method. The susceptible area distributed in landslide susceptibility map is 7.57 % of the area under very high, 14.28 % of the area comes under high, and 23.99, 30.75, and 23.41 of the area occupies as moderate, low, very low, respectively.

Statistical index

To perform the statistical index modeling, the resultant weights for each thematic map for the SI model were calculated in ArcGIS 10.0 and Microsoft Excel, and the results are shown in Table 2. The higher resultant weight, the higher is the possibility that a mass movement occurs within the area covered by the considered class. These weights were analyzed by using the weighted sum option in the spatial analyst tools of ArcGIS 10.0 to get the final Landslide susceptibility map (Fig. 6). In this study, Landslide susceptibility map was classified into five categories by using the natural break method of ArcGIS. These categories include five classes of very low (−9.42–−5.06), low (−5.06–−2.69), moderate (−2.69–−0.38), high (−0.38–1.93), and very high (1.93–6.93). The area percentages in the very low, low, moderate, high, and very high landslide susceptibility classes are 20.49, 26.80, 21.66, 18.84, and 12.21 %, respectively.

Weights-of-evidence model

Every parameter map is crossed with the landslide inventory map based on the weights-of-evidence model using the ArcGIS 10.0 software, and the density of the landslide in each class is calculated. The resultant weights for each thematic map for the WoE model are given in Table 2. For getting the final LSI map (Fig. 7), these weights were analyzed by using the weighted sum option in the spatial analyst tools of ArcGIS 10.0. The final calculated LSI values of the study area for WoE model range from about −25.40 to 34.67. In this study,

Table 1 Description of geological units of the study area

No.	Code	Formation	Lithology	Geological age
1	Q ₄	–	Sand, gravel, silty clay	Quaternary
2	Q ₃	–	Loess	Quaternary
3	Q ₂	–	Loess	Quaternary
4	Q ₁	–	Loess	Quaternary
5	N ₂	–	Glutenite, sandstone, siltstone	Neogene
6	K _{1Lh}	Luohandong	Sandstone, siltstone, mudstone	Early Cretaceous
	K _{1h}	Huanhehuachi	Sandstone, siltstone, mudstone	Early Cretaceous
	K _{1L}	Luohe	Glutenite, sandstone	Early Cretaceous
	K _{1y}	Yijun	Glutenite	Early Cretaceous
7	J _{3f}	Fenfanghe	Glutenite, sandstone, siltstone	Late Jurassic
	J _{2z}	Zhiluo	Glutenite, siltstone	Middle Jurassic
8	P ₁	–	Sandstone, shale	Early Permian
9	O _{1–2}	–	Limestone, dolomite	Early- Middle Ordovician

Table 2 Spatial relationship between each landslide conditioning factor and landslide by FR, SI and WoE models

Factors	Classes	Percentage of landslide (%)	Percentage of domain (%)	FR	SI	W^-	C	$S^2(W^+)$	$S^2(W^-)$	$S(C)$	$S/S(C)$
Slope angle (°)	0–7	30.36	32.51	0.93	-0.07	0.03	-0.10	0.06	0.03	0.29	-0.34
	7–14	33.93	35.59	0.95	-0.05	0.03	-0.07	0.05	0.03	0.28	-0.26
	14–21	30.36	26.18	1.16	0.15	-0.06	0.21	0.06	0.03	0.29	0.71
	21–28	5.36	5.42	0.99	-0.01	0.00	-0.01	0.33	0.02	0.59	-0.02
	28–38	0.00	0.30	0.00	0.00	0.00	0.00	0.00	0.02	0.00	0.00
Slope aspect	Flat	0.00	6.16	0.00	0.00	0.06	0.00	0.00	0.02	0.00	0.00
	North	16.07	9.62	1.67	0.51	-0.07	0.59	0.11	0.02	0.36	1.61
	Northeast	12.50	10.23	1.22	0.20	-0.03	0.23	0.14	0.02	0.40	0.56
	East	14.29	11.21	1.27	0.24	-0.04	0.28	0.13	0.02	0.38	0.73
	Southeast	10.71	13.37	0.80	-0.22	0.03	-0.25	0.17	0.02	0.43	-0.58
	South	7.14	9.77	0.73	-0.31	0.03	-0.34	0.25	0.02	0.52	-0.66
	Southwest	16.07	13.16	1.22	0.20	-0.03	0.23	0.11	0.02	0.36	0.64
	West	5.36	13.30	0.40	-0.91	0.09	-1.00	0.33	0.02	0.59	-1.68
	Northwest	17.86	13.19	1.35	0.30	-0.06	0.36	0.10	0.02	0.35	1.03
	Curvature	<-0.05	46.43	36.59	1.27	0.24	-0.17	0.41	0.04	0.03	0.27
-0.05–0.05		23.21	26.92	0.86	-0.15	0.05	-0.20	0.08	0.02	0.32	-0.62
>0.05		30.36	36.48	0.83	-0.18	0.09	-0.28	0.06	0.03	0.29	-0.95
Plan curvature	<-0.05	28.57	27.19	1.05	0.05	-0.02	0.07	0.06	0.03	0.30	0.23
	-0.05–0.05	50.00	43.00	1.16	0.15	-0.13	0.28	0.04	0.04	0.27	1.06
	>0.05	21.43	29.81	0.72	-0.33	0.11	-0.44	0.08	0.02	0.33	-1.36
Profile curvature	<-0.05	26.79	30.49	0.88	-0.13	0.05	-0.18	0.07	0.02	0.30	-0.60
	-0.05–0.05	26.79	37.24	0.72	-0.33	0.15	-0.48	0.07	0.02	0.30	-1.60
	>0.05	46.43	32.27	1.44	0.36	-0.23	0.60	0.04	0.03	0.27	2.23
Altitude (m)	720–850	41.07	11.95	3.44	1.23	-0.40	1.64	0.04	0.03	0.27	6.02
	850–1000	46.43	24.96	1.86	0.62	-0.34	0.96	0.04	0.03	0.27	3.57
	1000–1150	7.14	22.91	0.31	-1.17	0.19	-1.35	0.25	0.02	0.52	-2.60
	1150–1300	3.57	25.48	0.14	-1.97	0.26	-2.22	0.50	0.02	0.72	-3.09
	1300–1560	1.79	14.69	0.12	-2.11	0.14	-2.25	1.00	0.02	1.01	-2.23
Distance to faults (m)	0–2000	51.79	26.72	1.94	0.66	-0.42	1.08	0.03	0.04	0.27	4.04
	2000–4000	16.07	14.09	1.14	0.13	-0.02	0.16	0.11	0.02	0.36	0.43
	4000–6000	14.29	10.78	1.33	0.28	-0.04	0.32	0.13	0.02	0.38	0.84
	6000–8000	8.93	7.89	1.13	0.12	-0.01	0.14	0.20	0.02	0.47	0.29
	>8000	8.93	40.52	0.22	-1.51	0.43	-1.94	0.20	0.02	0.47	-4.14
Distance to rivers (m)	0–200	46.43	22.26	2.09	0.73	-0.37	1.11	0.04	0.03	0.27	4.13
	200–400	14.29	18.01	0.79	-0.23	0.04	-0.28	0.13	0.02	0.38	-0.72
	400–600	8.93	14.14	0.63	-0.46	0.06	-0.52	0.20	0.02	0.47	-1.11
	600–800	7.14	11.30	0.63	-0.46	0.05	-0.50	0.25	0.02	0.52	-0.97
	>800	23.21	34.29	0.68	-0.39	0.16	-0.55	0.08	0.02	0.32	-1.72
Distance to roads (m)	0–1000	53.57	36.73	1.46	0.38	-0.31	0.69	0.03	0.04	0.27	2.56
	1000–2000	14.29	23.90	0.60	-0.51	0.12	-0.63	0.13	0.02	0.38	-1.66
	2000–3000	23.21	17.75	1.31	0.27	-0.07	0.34	0.08	0.02	0.32	1.06
	3000–4000	8.93	11.81	0.76	-0.28	0.03	-0.31	0.20	0.02	0.47	-0.67
	>4000	0.00	9.81	0.00	0.00	0.10	0.00	0.00	0.02	0.00	0.00
STI	<3	12.50	24.60	0.51	-0.68	0.15	-0.83	0.14	0.02	0.40	-2.04
	3–9	28.57	26.81	1.07	0.06	-0.02	0.09	0.06	0.03	0.30	0.30
	9–15	16.07	19.98	0.80	-0.22	0.05	-0.27	0.11	0.02	0.36	-0.73
	>15	42.86	28.60	1.50	0.40	-0.22	0.63	0.04	0.03	0.27	2.32
SPI	<5	5.36	14.80	0.36	-1.02	0.11	-1.12	0.33	0.02	0.59	-1.89

Table 2 (continued)

Factors	Classes	Percentage of landslide (%)	Percentage of domain (%)	FR	SI	W^-	C	$S^2(W^+)$	$S^2(W^-)$	$S(C)$	$S/S(C)$
TWI	5–10	5.36	10.85	0.49	-0.71	0.06	-0.77	0.33	0.02	0.59	-1.29
	10–40	32.14	34.55	0.93	-0.07	0.04	-0.11	0.06	0.03	0.29	-0.38
	>40	57.14	39.81	1.44	0.36	-0.34	0.70	0.03	0.04	0.27	2.60
	<7	55.36	55.01	1.01	0.01	-0.01	0.01	0.03	0.04	0.27	0.05
	7–10	26.79	30.12	0.89	-0.12	0.05	-0.16	0.07	0.02	0.30	-0.54
	10–13	10.71	6.28	1.71	0.53	-0.05	0.58	0.17	0.02	0.43	1.35
	>13	7.14	8.59	0.83	-0.18	0.02	-0.20	0.25	0.02	0.52	-0.39
Lithology	1	3.57	4.41	0.81	-0.21	0.01	-0.22	0.50	0.02	0.72	-0.31
	2	30.36	17.11	1.77	0.57	-0.17	0.75	0.06	0.03	0.29	2.57
	3	39.29	10.99	3.58	1.27	-0.38	1.66	0.05	0.03	0.27	6.06
	4	3.57	14.29	0.25	-1.39	0.12	-1.50	0.50	0.02	0.72	-2.09
	5	1.79	0.31	5.68	1.74	-0.01	1.75	1.00	0.02	1.01	1.74
	6	12.50	45.68	0.27	-1.30	0.48	-1.77	0.14	0.02	0.40	-4.39
	7	3.57	2.13	1.68	0.52	-0.01	0.53	0.50	0.02	0.72	0.74
	8	1.79	0.71	2.51	0.92	-0.01	0.93	1.00	0.02	1.01	0.92
	9	3.57	4.37	0.82	-0.20	0.01	-0.21	0.50	0.02	0.72	-0.29

the LSI on the produced maps was grouped into five classes (very low, low, moderate, high, and very high) using the natural break method. According to this model, 8.94 % of the area is exposed to a very high susceptibility, and 17.14, 24.98, 25.87, and 23.07 % occupy high, moderate, low, and very low, respectively.

Validation of the models used

Validation of landslide susceptibility models is an essential requirement to check the predictive capabilities of the landslide susceptibility map produced (Chung and Fabbri 2003). The landslide susceptibility maps derived by three models

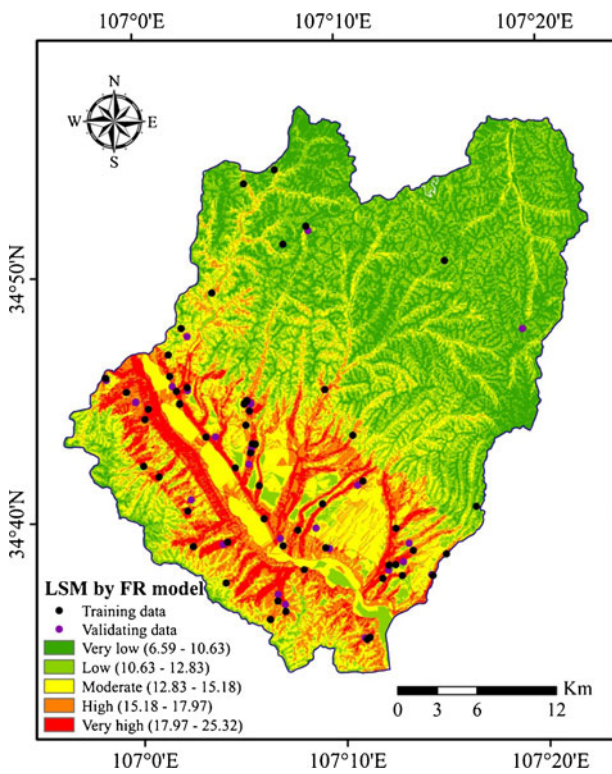


Fig. 5 Landslide susceptibility map derived from the FR model

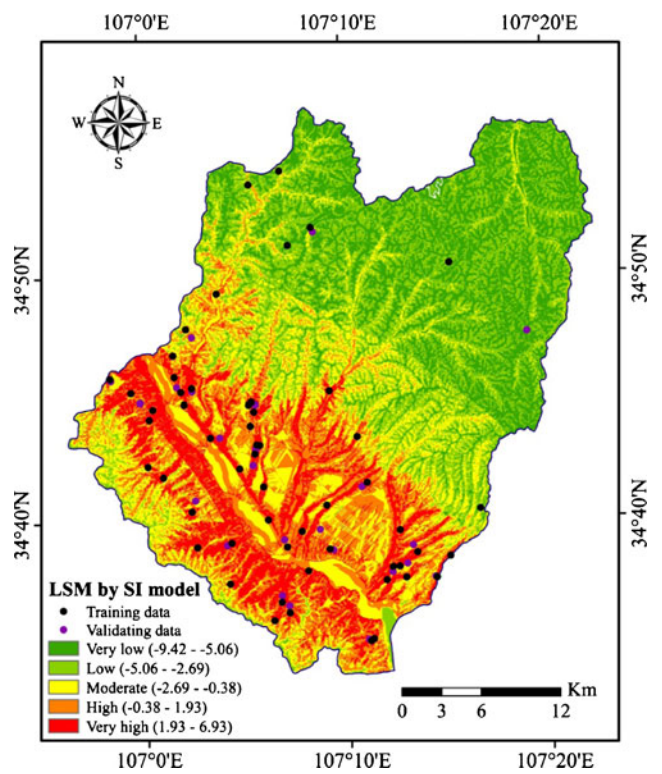


Fig. 6 Landslide susceptibility map derived from the SI model

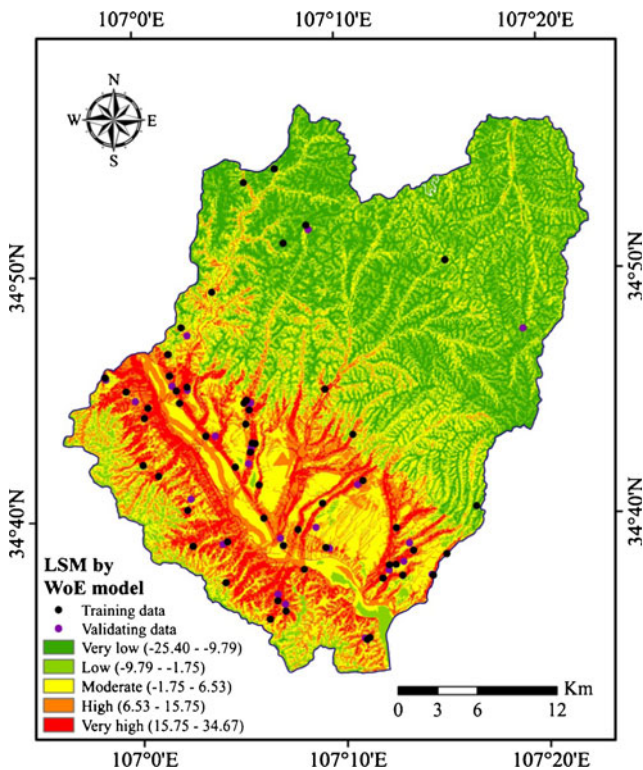


Fig. 7 Landslide susceptibility map derived from the WoE model

were tested by comparison of existing landslide data and landslide susceptibility analysis results for the study area. For this, the total landslides observed in the study area were split into two groups, 56 (70 %) landslides were randomly selected from the total 81 landslides as the training data, and the remaining 25 (30 %) landslides were kept for validation propose. In this study, the prediction capability of a landslide susceptibility model is usually estimated using area under the curve (AUC) methods. The rate curves were created, and their areas under the curve (AUC) used to qualitatively assess the prediction accuracy, were calculated (Fig. 8). The rate

explains how well the model and controlling factors predict the landslide. The model with the highest AUC is considered to be the best.

The success rate curve was obtained by comparing the landslide training data with the susceptibility maps (Fig. 8a). The AUC plot assessment results showed that the AUC values were 0.8362, 0.8345, and 0.8251 for FR, SI, and WoE models, and the training accuracy were 83.62, 83.45, and 82.51 %, respectively. The prediction-rate curve, obtained by comparing the landslide validation data with the susceptibility map (Fig. 8b), showed that the AUC values were 0.7940, 0.7935, and 0.7853 for FR, SI, and WoE models, and the prediction accuracy was 79.40, 79.35, and 78.53 %, respectively. The results of the AUC evaluation show that both the success rate and prediction rate curve have almost similar result. All the models employed in this study showed reasonably high prediction accuracy and can be used for the spatial prediction of landslide hazard analysis of the study area. On the other hand, the map produced by FR model exhibited the best result for landslide susceptibility mapping in the study area.

Conclusions

Generally, landslides are unpredictable; however, the susceptibility assessment of landslide occurrence can be determined using different GIS-based methods. In this study, we used three statistical models, such as frequency ratio (FR), statistical index (SI), and index of entropy (WoE) models, to produce landslide susceptibility maps for the Qianyang County of Baoji City, China. Their performances were compared by using area under the curve (AUC) methods. For generating landslide susceptibility maps in the study region, 13 landslide-conditioning factors were considered as slope angle, slope aspect, curvature, plan curvature, profile curvature,

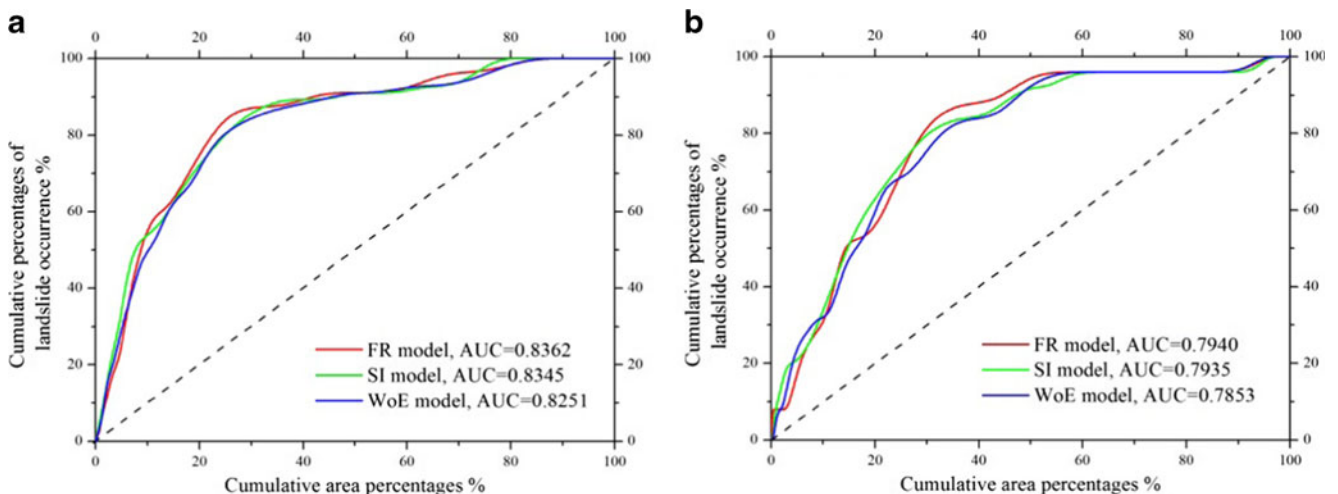


Fig. 8 AUC representing quality of the model

altitude, distance to faults, distance to rivers, distance to roads, STI, SPI, TWI, and lithology, for which maps were derived using various GIS tools. The selection of these factors was based on consideration of relevance, availability, and scale of data that was available for the study area. In this process, a total of 81 landslides were identified and mapped. Out of which, 56 (70 %) were randomly selected for generating a model, and the remaining 25 (30 %) were used for validation purposes. In this study, five landslide susceptibility classes, i.e., very low, low, moderate, high, and very high susceptibility for landsliding, were derived with natural break method. The verification results showed that the landslide susceptibility map generated by the FR model has the highest prediction accuracy (79.40 %), followed by the SI model (79.35 %), and the WoE model (78.53 %). Success rate curve gives similar result, with FR model the highest AUC value (83.62 %), followed by the SI model (83.45 %), and the WoE model (82.51 %). This shows that the three models have been applied successfully to the production of landslide susceptibility maps. The landslide susceptibility maps provide valuable information on the slope stability in study area, which may be used for infrastructure planning, land use, engineering, and hazard mitigation design. Also, it is helpful that the similar method can be used elsewhere where the similar landslide occurrence conditions.

Acknowledgments The authors are thankful to two anonymous reviewers for their valuable comments which were very useful in bringing the manuscript into its present form.

References

- Akgun A (2012) A comparison of landslide susceptibility maps produced by logistic regression, multi-criteria decision, and likelihood ratio methods: a case study at Izmir, Turkey. *Landslides* 9:93–106
- Akgun A, Turk N (2010) Landslide susceptibility mapping for Ayvalik (Western Turkey) 379 and its vicinity by multicriteria decision analysis. *Environ Earth Sci* 61(3):595–611
- Akgun A, Kincal C, Pradhan B (2012a) Application of remote sensing data and GIS for landslide risk assessment as an environmental threat to Izmir city (West Turkey). *Environ Monit Assess* 184: 5453–5470
- Akgun A, Sezer EA, Nefeslioglu HA, Gokceoglu C, Pradhan B (2012b) An easy-to-use MATLAB program (MamLand) for the assessment of landslide susceptibility using a Mamdani fuzzy algorithm. *Comput Geosci* 38(1):23–34
- Aleotti P, Chowdhury R (1999) Landslide hazard assessment: summary review and new perspectives. *Bull Eng Geol Environ* 58(1):21–44
- Baeza C, Corominas J (2001) Assessment of shallow landslide susceptibility by means of multivariate statistical techniques. *Earth Surf Process Landf* 26:1251–1263
- Bathrellos GD, Kalivas DP, Skilodimou HD (2009) GIS-based landslide susceptibility mapping models applied to natural and urban planning in Trikala, Central Greece. *Estud Geol* 65(1):49–65
- Bathrellos GD, Gaki-Papanastassiou K, Skilodimou HD, Papanastassiou D, Chousianitis KG (2012) Potential suitability for urban planning and industry development by using natural hazard maps and geological—geomorphological parameters. *Environ Earth Sci* 66(2):537–548
- Bathrellos GD, Gaki-Papanastassiou K, Skilodimou HD, Skianis GA, Chousianitis KG (2013) Assessment of rural community and agricultural development using geomorphological—geological factors and GIS in the Trikala prefecture (Central Greece). *Stoch Env Res Risk A* 27(2):573–588
- Bourenane H, Bouhadad Y, Guettouche MS, Braham M (2015) GIS-based landslide susceptibility zonation using bivariate statistical and expert approaches in the city of Constantine (Northeast Algeria). *Bull Eng Geol Environ* 74(2):337–355
- Bui DT, Lofman O, Revhaug I, Dick O (2011) Landslide susceptibility analysis in the Hoa Binh province of Vietnam using statistical index and logistic regression. *Nat Hazards* 59:1413–1444
- C.H. of China geological environment information sit (CIGEM) (2014) <http://www.cigem.gov.cn/>
- C.H. of China Meteorological Administration(CMA) (2014) http://cdc.cma.gov.cn/cdc_en/home.dd
- Catani F, Lagomarsino S, Segoni S, Tofani V (2013) Landslide susceptibility estimation by random forests technique: sensitivity and scaling issues. *Nat Hazards Earth Syst Sci* 13:2815–2831
- Cevik E, Topal T (2003) GIS-based landslide susceptibility mapping for a problematic segment of the natural gas pipeline, Hendek (Turkey). *Environ Geol* 44:949–962
- Chung CJF, Fabbri AG (2003) Validation of spatial prediction models for landslide hazard mapping. *Nat Hazards* 30(3):451–472
- Clerici A, Perego S, Tellini C, Vescovi P (2002) A procedure for landslide susceptibility zonation by the conditional analysis method. *Geomorphology* 48:349–364
- Clerici A, Perego S, Tellini C, Vescovi P (2006) A GIS-based automated procedure for landslide susceptibility mapping by the conditional analysis method: the Baganza valley case study (Italian Northern Apennines). *Environ Geol* 50:941–961
- Conforti M, Aucelli PP, Robustelli G, Scarciglia F (2011) Geomorphology and GIS analysis for mapping gully erosion susceptibility in the Turbolo stream catchment (Northern Calabria, Italy). *Nat Hazards* 56(3):881–898
- Dahal RK, Hasegawa S, Nonomura A, Yamanaka M, Masuda T, Nishino K (2008) GIS-based weights-of-evidence modelling of rainfall-induced landslides in small catchments for landslide susceptibility mapping. *Environ Geol* 54(2):311–324
- Demir G, Aytekin M, Akgun A (2015) Landslide susceptibility mapping by frequency ratio and logistic regression methods: an example from Niksar-Resadiye (Tokat, Turkey). *Arab J Geosci* 8(3):1801–1812
- Devkota KC, Regmi AD, Pourghasemi HR, Yoshida K, Pradhan B, Ryu IC, Dhital MR, Althuwaynee OF (2013) Landslide susceptibility mapping using certainty factor, index of entropy and logistic regression models in GIS and their comparison at Mugling-Narayanghat road section in Nepal Himalaya. *Nat Hazards* 65(1):135–165
- Donati L, Turrini MC (2002) An objective method to rank the importance of the factors predisposing to landslides with the GIS methodology: application to an area of the Apennines (Valnerina; Perugia, Italy). *Eng Geol* 63:277–289
- Ercanoglu M, Gokceoglu C, van Asch TWJ (2004) Landslide susceptibility zoning north of Yenice (NW Turkey) by multivariate statistical techniques. *Nat Hazards* 32:1–23
- Fell R, Corominas J, Bonnard C, Cascini L, Leroi E, Savage W (2008) Guidelines for landslide susceptibility, hazard and risk zoning for land use planning. *Eng Geol* 102:85–98
- Grozavu A, Plescan S, Patriche CV, Margarint MC, Rosca B (2013) Landslide Susceptibility Assessment: GIS Application to a Complex Mountainous Environment. *The Carpathians: Integrating Nature and Society Towards Sustainability*. *Environ Sci Eng*, pp 31–44

- Guettouche MS (2013) Modeling and risk assessment of landslides using fuzzy logic. Application on the slopes of the Algerian tell (Algeria). *Arab J Geosci* 6:3163–3173
- Jaupaj O, Lateltin O, Lamaj M (2014). Landslide Susceptibility of Kavaja, Albania. In *Landslide Science for a Safer Geoenvironment* pp. 351–356
- Jibson WR, Edwin LH, John AM (2000) A method for producing digital probabilistic seismic landslide hazard maps. *Eng Geol* 58:271–289
- Kayastha P (2015) Landslide susceptibility mapping and factor effect analysis using frequency ratio in a catchment scale: a case study from Garuwa sub-basin, East Nepal. *Arab J Geosci*. doi:10.1007/s12517-015-1831-6
- Kayastha P, Dhital MR, De Smedt F (2013) Application of analytical hierarchy process (AHP) for landslide susceptibility mapping: a case study from the Tinau watershed, west Nepal. *Comput Geosci* 52: 398–408
- Kouli M, Loupasakis C, Soupios P, Rozos D, Vallianatos F (2014) Landslide susceptibility mapping by comparing the WLC and WofE multi-criteria methods in the West Crete Island, Greece. *Environ Earth Sci* 72(12):5197–5219
- Kundu S, Saha AK, Sharma DC, Pant CC (2013) Remote sensing and GIS based landslide susceptibility assessment using binary logistic regression model: a case study in the Ganeshganga watershed, Himalayas. *J Indian Soc Remote Sens* 41(3):697–709
- Lee S, Choi U (2003) Development of GIS-based geological hazard information system and its application for landslide analysis in Korea. *Geosci J* 7:243–252
- Lee S, Min K (2001) Statistical analysis of landslide susceptibility at Youngin, Korea. *Environ Geol* 40:1095–1113
- Lee S, Talib JA (2005) Probabilistic landslide susceptibility and factor effect analysis. *Environ Geol* 47:982–990
- Lee S, Choi J, Min K (2004a) Probabilistic landslide hazard mapping using GIS and remote sensing data at Boeun, Korea. *Int J Remote Sens* 25:2037–2052
- Lee S, Ryu JH, Won JS, Park HJ (2004b) Determination and application of the weights for landslide susceptibility mapping using an artificial neural network. *Eng Geol* 71:289–302
- Liu C, Li W, Wu H, Lu P, Sang K, Sun W, Chen W, Hong Y, Li R (2013) Susceptibility evaluation and mapping of China's landslides based on multi-source data. *Nat Hazards* 69(3):1477–1495
- Luzi L, Pergalani F, Terlien MTJ (2000) Slope vulnerability to earthquakes at subregional scale, using probabilistic techniques and geographic information systems. *Eng Geol* 58:313–336
- Marjanović M, Kovačević M, Bajat B, Voženilek V (2011) Landslide susceptibility assessment using SVM machine learning algorithm. *Eng Geol* 123:225–234
- Mihaela C, Martin B, Marta CJ, Marius V (2011) Landslide susceptibility assessment using the bivariate statistical analysis and the index of entropy in the Sibiciu Basin (Romania). *Environ Earth Sci* 63:397–406
- Nefeslioglu HA, Duman TY, Durmaz S (2008) Landslide susceptibility mapping for a part of tectonic Kelkit Valley (Eastern Black Sea region of Turkey). *Geomorphology* 94(3):401–418
- Oh HJ, Lee S (2011) Landslide susceptibility mapping on Panaon Island, Philippines using a geographic information system. *Environ Earth Sci* 62(5):935–951
- Ozdemir A, Altural T (2013) A comparative study of frequency ratio, weights of evidence and logistic regression methods for landslide susceptibility mapping: Sultan Mountains, SW Turkey. *J Asian Earth Sci* 64:180–197
- Pareek N, Sharma ML, Arora MK (2010) Impact of seismic factors on landslide susceptibility zonation: a case study in part of Indian Himalayas. *Landslides* 7(2):191–201
- Pareek N, Sharma ML, Arora MK, Pal S (2013) Inclusion of earthquake strong ground motion in a geographic information system-based landslide susceptibility zonation in Garhwal Himalayas. *Nat Hazards* 65(1):739–765
- Parise M, Jibson WR (2000) A seismic landslide susceptibility rating of geologic units based on analysis of characteristics of landslides triggered by the 17 January, 1994 Northridge, California earthquake. *Eng Geol* 58:251–270
- Park S, Choi C, Kim B, Kim J (2013) Landslide susceptibility mapping using frequency ratio, analytic hierarchy process, logistic regression, and artificial neural network methods at the Inje area, Korea. *Environ Earth Sci* 68:1443–1464
- Poudyal CP, Chang C, Oh HJ, Lee S (2010) Landslide susceptibility maps comparing frequency ratio and artificial neural networks: a case study from the Nepal Himalaya. *Environ Earth Sci* 61(5):1049–1064
- Pourghasemi HR, Pradhan B, Gokceoglu C (2012) Application of fuzzy logic and analytical hierarchy process (AHP) to landslide susceptibility mapping at Haraz watershed, Iran. *Nat Hazards* 63:965–996
- Pourghasemi HR, Jirandeh AG, Pradhan B, Xu C, Gokceoglu C (2013a) Landslide susceptibility mapping using support vector machine and GIS at the Golestan province, Iran. *J Earth Syst Sci* 122(2):349–369
- Pourghasemi HR, Moradi HR, Fatemi Aghda SM (2013b) Landslide susceptibility mapping by binary logistic regression, analytical hierarchy process, and statistical index models and assessment of their performances. *Nat Hazards* 69:749–779
- Pourghasemi HR, Pradhan B, Gokceoglu C, Deylami Moezzi K (2013c) A comparative assessment of prediction capabilities of Dempster-Shafer and weights-of-evidence models in landslide susceptibility mapping using GIS. *Geomat, Nat Hazards Risk* 4(2):93–118
- Pourghasemi HR, Pradhan B, Gokceoglu C, Mohammadi M, Moradi HR (2013d) Application of weights-of-evidence and certainty factor models and their comparison in landslide susceptibility mapping at Haraz watershed, Iran. *Arab J Geosci* 6:2351–2365
- Pradhan B (2013) A comparative study on the predictive ability of the decision tree, support vector machine and neuro-fuzzy models in landslide susceptibility mapping using GIS. *Comput Geosci* 51: 350–365
- Pradhan B, Lee S (2010) Landslide susceptibility assessment and factor effect analysis: back-propagation artificial neural networks and their comparison with frequency ratio and bivariate logistic regression modeling. *Environ Model Softw* 25(6):747–759
- Pradhan B, Youssef AM (2010) Manifestation of remote sensing data and GIS on landslide hazard analysis using spatial-based statistical models. *Arab J Geosci* 3(3):319–326
- Pradhan B, Singh RP, Buchroithner MF (2006) Estimation of stress and its use in evaluation of landslide prone regions using remote sensing data. *Adv Space Res* 37:698–709
- Pradhan B, Mansor S, Pirasteh S, Buchroithner M (2011) Landslide hazard and risk analyses at a landslide prone catchment area using statistical based geospatial model. *Int J Remote Sens* 32(14):4075–4087
- Regmi AD, Devkota KC, Yoshida K, Pradhan B, Pourghasemi HR, Kumamoto T, Akgun A (2014) Application of frequency ratio, statistical index, and weights-of-evidence models and their comparison in landslide susceptibility mapping in Central Nepal Himalaya. *Arab J Geosci* 7(2):725–742
- Rozos D, Bathrellos GD, Skilodimou HD (2011) Comparison of the implementation of rock engineering system (RES) and analytic hierarchy process (AHP) methods, based on landslide susceptibility maps, compiled in GIS environment. A case study from the Eastern Achaia County of Peloponnesus, Greece. *Environ Earth Sci* 63(1): 49–63
- Saha AK, Gupta RP, Sarkar I, Arora MK, Csaplovics E (2005) An approach for GIS-based statistical landslide susceptibility zonation with a case study in the Himalayas. *Landslides* 2:61–69
- Sharma LP, Patel N, Ghose MK, Debnath P (2013) Synergistic application of fuzzy logic and geo-informatics for landslide vulnerability

- zonation—a case study in Sikkim Himalayas, India. *Appl Geomat* 5: 271–284
- Sujatha ER, Kumaravel P, Rajamanickam GV (2014) Assessing landslide susceptibility using Bayesian probability-based weight of evidence model. *Bull Eng Geol Environ* 73(1):147–161
- Tay LT, Lateh H, Hossain MK, Kamil, AA (2014) Landslide Hazard Mapping Using a Poisson Distribution: A Case Study in Penang Island, Malaysia. In: *Landslide Science for a Safer Geoenvironment* (pp. 521–525). Springer International Publishing
- Tunusluoglu MC, Gokceoglu C, Nefeslioglu HA, Sonmez H (2007) Extraction of potential debris source areas by logistic regression technique: a case study from Barla, Besparmak and Kapi mountains (NW Taurids, Turkey). *Environ Geol* 54:9–22
- Van Westen CJ, Rengers N, Soeters R (2003) Use of geomorphological information in indirect landslide susceptibility assessment. *Nat Hazards* 30(3):399–419
- Van Westen CJ, Van Asch TW, Soeters R (2006) Landslide hazard and risk zonation—why is it still so difficult? *Bull Eng Geol Environ* 65(2):167–184
- Vijith H, Madhu G (2008) Estimating potential landslide sites of anupland sub-atershed in Western Ghat's of Kerala (India) through frequency ratio and GIS. *Environ Geol* 55:1397–1405
- Xu C, Dai FC, Xu X, Lee YH (2012a) GIS-based support vector machine modeling of earthquake-triggered landslide susceptibility in the Jianjiang River watershed, China. *Geomorphology* 145–146:70–80
- Xu C, Xu XW, Dai FC, Saraf AK (2012b) Comparison of different models for susceptibility mapping of earthquake triggered landslides related with the 2008 Wenchuan earthquake in China. *Comput Geosci* 46:317–329
- Yilmaz I (2009a) A case study from Koyulhisar (Sivas-Turkey) for landslide susceptibility mapping by artificial neural networks. *Bull Eng Geol Environ* 68(3):297–306
- Yilmaz I (2009b) Landslide susceptibility mapping using frequency ratio, logistic regression, artificial neural networks and their comparison: a case study from Kat landslides (Tokat-Turkey). *Comput Geosci* 35(6):1125–1138
- Yilmaz I (2010a) The effect of the sampling strategies on the landslide susceptibility mapping by conditional probability (CP) and artificial neural network (ANN). *Environ Earth Sci* 60:505–519
- Yilmaz I (2010b) Comparison of landslide susceptibility mapping methodologies for Koyulhisar, Turkey: conditional probability, logistic regression, artificial neural networks, and support vector machine. *Environ Earth Sci* 61:821–836
- Yilmaz C, Topal T, Suzen ML (2012) GIS-based landslide susceptibility mapping using bivariate statistical analysis in Devrek (Zonguldak-Turkey). *Environ Earth Sci* 65:2161–2178
- Youssef AM, Pradhan B, Gaber AFD, Buchroithner MF (2009) Geomorphological hazard analysis along the Egyptian Red Sea coast between Safaga and Quseir. *Nat Hazards Earth Syst Sci* 9: 751–766
- Youssef AM, Pradhan B, Sabtan AA, El-Harbi HM (2012) Coupling of remote sensing data aided with field investigations for geological hazards assessment in Jazan area, Kingdom of Saudi Arabia. *Environ Earth Sci* 65(1):119–130
- Youssef AM, Pradhan B, Al-Harhi SG (2014a) Assessment of rock slope stability and structurally controlled failures along Samma escarpment road, Asir Region (Saudi Arabia). *Arab J Geosci*. doi:10.1007/s12517-014-1719-x
- Youssef AM, Pradhan B, Sefry SA, Abu Abdullah MM (2014b) Use of geological and geomorphological parameters in potential suitability assessment for urban planning development at Wadi Al-Asla basin, Jeddah, Kingdom of Saudi Arabia. *Arab J Geosci*. doi:10.1007/s12517-014-1663-9
- Youssef AM, Pradhan B, Al-Kathery M, Bathrellos GD, Skilodimou HD (2015a) Assessment of rockfall hazard at Al-Noor Mountain, Makkah city (Saudi Arabia) using spatio-temporal remote sensing data and field investigation. *J Afr Earth Sci* 101:309–321
- Youssef AM, Pradhan B, Jebur MN, El-Harbi HM (2015b) Landslide susceptibility mapping using ensemble bivariate and multivariate statistical models in Fayfa area, Saudi Arabia. *Environ Earth Sci* 73(7):3745–3761
- Zhou CH, Lee CF, Li J, Xu ZW (2002) On the spatial relationship between landslides and causative factors on Lantau Island, Hong Kong. *Geomorphology* 43:197–207